Biochimica et Biophysica Acta, 599 (1980) 202—213

BBA 78752

AN ALLOSTERIC PORE MODEL FOR SUGAR TRANSPORT IN HUMAN ERYTHROCYTES

G.D. HOLMAN

The Department of Biochemistry, The University of Bath, Bath BA2 7AY (U.K.)

(Received November 5th, 1979)

Key words: Allosteric pore; Sugar transport; Transport gating; (Human erythrocyte)

Summary

Glucose transport in human erythrocytes is characterized by a marked asymmetry in the V and K_m values for entry and for exit. In addition, they show a high K_m and a high V for equilibrium exchange but low K_m values for infinite *cis* and for infinite *trans* exit and entry. An allosteric pore model has been proposed to account for these characteristics. In this model, substrate-induced conformational changes destabilize the interfaces between protein subunits (the pore gates).

Pores doubly occupied from inside destabilize the transport gates and result in high K_m and high V transport parameters. This effect is less marked when pores are doubly occupied from outside and therefore transport asymmetry results.

Introduction

The huge variety of experimental approaches and resultant kinetic tests that are possible when studying sugar transport have repeatedly been devastating in their rejection of the various kinetic models that have been proposed to account for sugar transport. Since inconsistency with any single test is sufficient to reject any model, the following failures have been noted [17,19]. The observation of asymmetry in the V values for entry and exit of sugars is inconsistent with the symmetric carrier [1], the symmetric pore model [2], the tetramer model [3] and the introverting hemi port model [4]. The observation of a low internal K_m in the infinite *cis* entry and the infinite *trans* exit experiments [14,17] is inconsistent with the asymmetric carrier model [5], the asymmetric carrier with unstirred layers [6] and a model with two antiparallel asymmetric carriers [7]. The observation of a high K_m inside erythrocyte

ghosts (Taylor, L.P. and Holman, G.D., unpublished results) is inconsistent with a symmetric pore model in which kinetic asymmetrics are due to formation of, and dissociation from, a sugar-haemoglobin complex [19].

Because there is no longer a model that is consistent with all the data we propose a new model.

An allosteric pore model

The models that have been advanced to account for sugar transport in recent years can be divided into sequential-occupancy and simultaneous-occupancy models. Sequential models have as their central assumption the principle that the substrate binding site is never simultaneously exposed to internal and to external solutions. The distinction between sequential pores and sequential carriers is not a useful one since both have the same kinetic formulation. Simultaneous models, on the other hand, have binding sites that can accept substrate at internal and at external sites together. Another important feature of such models is that there must be sufficient space within the transport protein for molecules entering at opposite sides to bypass one another. Molecules may pass each other within internal cavities in the centre of the protein or at the entrance to the protein (the gates). This type of model is consistent with current views that the transport proteins are intrinsic and span the membrane. Such a protein would probably be at least $2.5 \cdot 10^5$ Å^3 and since not all the space in the protein will be occupied by amino acids of the peptide chains it is perfectly reasonable to anticipate that two sugars, each approx. $1.25 \cdot 10^2$ Å^3, could pass one another somewhere. These models have developed from concepts advanced by Naftalin [2] and by Lieb and Stein [3].

As an extension to the simultaneous-occupancy models, we have examined the properties of an allosteric pore model. We have followed closely the theoretical analysis of the allosteric enzyme model of Koshland [8,9]. The symbols used for the conformational states of the protein also follow Koshland's work.

Some of the forms of the allosteric pore that are responsible for flux from outside of the cell are shown diagramatically in Scheme 1. All of the forms of

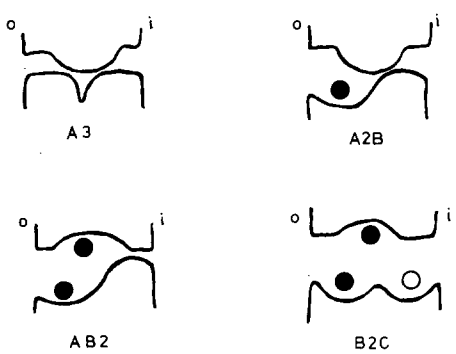

Scheme 1. A diagrammatic representation of the allosteric pore model. The pore can accept substrate from outside (●) and substrate from inside (○). A3 is the closed pore with stable subunit interfaces (transport gates). The A2B pore is occupied by a single substrate molecule from outside. The AB2 pore is occupied by two substrate molecules from outside. The B2C pore is occupied by two molecules from outside and by one molecule from inside.

the pore are shown schematically in Scheme 2. It is proposed that the protein

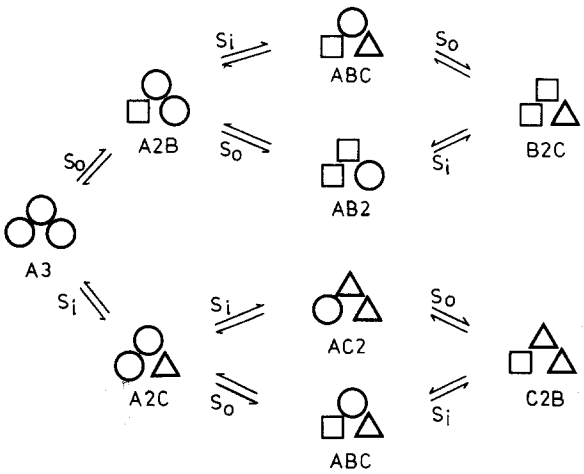

Scheme 2. A schematic representation of the allosteric pore showing all the proposed occupancy states. ○, A subunits; □, B subunits; △, C subunits. A linear arrangement of subunits is assumed.

spanning the membrane is composed of three subunits that are involved in transport (A3). Other subunits may be present but not directly involved in transport. The interactions between the subunits are symmetric in the closed pore but only two of the three subunits are available to substrate entering the pore from either outside or inside. A linear arrangement of subunits is assumed and only the outermost subunits are available to the first substrate molecule to bind. A subunits are empty, B subunits are occupied from outside and C subunits are occupied from inside. When the pore is occupied several conformational states can be identified.

(1) $A2BS_o$: The pore is occupied from outside by a single substrate molecule.

(2) $A2CS_i$: The pore is occupied from inside by a single substrate molecule.

(3) $ABCS_oS_i$: The pore is simultaneously occupied by one molecule from inside and one molecule from outside.

(4) $AC2S_i2$: The pore is occupied by two molecules from inside.

(5) $AB2S_o2$: The pore is occupied by two molecules from outside.

(6) $C2BS_i2S_o$: The pore is occupied by two molecules from inside and one molecule from outside.

(7) $B2CS_o2S_i$: The pore is occupied by two molecules from outside and one molecule from inside.

The total concentration of pores (T) will be:

$$T = [A3] + [A2BS_o] + [A2CS_i] + [ABCS_oS_i] + [AC2S_i2] + [AB2S_o2] + [C2BS_i2S_o] + [B2CS_o2S_i]$$

All conformational changes are substrate-induced. The binding of S_o changes the conformation of an A subunit to a new conformational state B. Similarly the binding of S_i causes an A → C conformational change.

The binding of S_o to an isolated B subunit is given by the association con-

stant (K_{S_o}) times the equilibrium constant for the A → B transition (K_b):

$$K_{S_o} \cdot K_b = \frac{[BS_o]}{[B] \cdot [S_o]} \cdot \frac{[B]}{[A]}$$

The binding of S_i to an isolated C subunit is given by K_{S_i} times the equilibrium constant for the A → C transition (K_c):

$$K_{S_i} \cdot K_c = \frac{[CS_i]}{[C] \cdot [S_i]} \cdot \frac{[C]}{[A]}$$

In addition one has to consider the interaction between subunits in the oligomeric pore. Six different interfaces will result from the interaction of A, B and C subunits (Scheme 2). These are AA, AB, AC, BC, BB and CC. The stability of these interfaces is given by equilibrium constants. These represent the tendency of the interfaces to dissociate (become unstable) relative to the dissociation or instability in the standard state A3.

$$K_{AB} = \frac{[AB]}{[AA]} \cdot \frac{[A]}{[B]}; \qquad K_{BB} = \frac{[BB]}{[AA]} \cdot \frac{[A] \cdot [A]}{[B] \cdot [B]}$$

$$K_{AC} = \frac{[AC]}{[AA]} \cdot \frac{[A]}{[C]}; \qquad K_{CC} = \frac{[CC]}{[AA]} \cdot \frac{[A] \cdot [A]}{[C] \cdot [C]}$$

$$K_{BC} = \frac{[BC]}{[AA]} \cdot \frac{[A] \cdot [A]}{[B] \cdot [C]}$$

The concentrations of the oligomeric states of the transport protein with a linear arrangement of subunits can now be given.

$$[A2BS_o] = [A3]\, K_{AB} K_b K_{S_o} [S_o]$$

$$[A2CS_i] = [A3]\, K_{AC} K_c K_{S_i} [S_i]$$

$$[ABCS_oS_i] = [A3]\, K_{AB} K_{AC} K_b K_{S_o} K_c K_{S_i} [S_o][S_i]$$

$$[AB2S_o2] = [A3]\, K_{BB} K_{AB} K_b^2 K_{S_o}^2 [S_o]^2$$

$$[AC2S_i2] = [A3]\, K_{CC} K_{AC} K_c^2 K_{S_i}^2 [S_i]^2$$

$$[B2CS_o2S_i] = [A3]\, K_{BC} K_{BB} K_b^2 K_{S_o}^2 K_c K_{S_i} [S_o]^2 [S_i]$$

$$[C2BS_i2S_o] = [A3]\, K_{BC} K_{CC} K_c^2 K_{S_i}^2 K_b K_{S_o} [S_i]^2 [S_o]$$

A triangular arrangement of subunits will give different equations. The major difference would be a BC subunit interaction in the expression for $[ABCS_oS_i]$. The fractional saturation of the pore is:

$$\Phi = ([A2BS_o] + [A2CS_i] + [ABCS_oS_i] + [AB2S_o2] + [AC2S_i2] + [B2CS_o2S_i] + [C2BS_i2S_o])([A3] + [A2BS_o] + [A2CS_i] + [ABCS_oS_i] + [AB2S_o2] + [AC2S_i2] + [B2CS_o2S_i] + [C2BS_i2S_o])^{-1}$$

In the case of sugar transport in intact erythrocytes it is assumed that the binding of S_o and S_i to isolated subunits is symmetric and that AB and AC subunit interactions are stable relative to the AA interaction. Introducing

experimentally measurable coefficients we obtain:

$$\Phi = \frac{[S_o] + [S_i] + K_x[S_o] \cdot [S_i] + K_{oo}[S_o]^2 + K_{ii}[S_i]^2 + K_{ooi}[S_o]^2[S_i] + K_{iio}[S_i]^2[S_o]}{\frac{1}{K_x} + [S_o] + [S_i] + K_x[S_o] \cdot [S_i] + K_{oo}[S_o]^2 + K_{ii}[S_i]^2 + K_{ooi}[S_o]^2[S_i] + K_{iio}[S_i]^2[S_o]} \quad (1)$$

where

$K_x = K_{S_o}K_b = K_{S_i}K_c$

$K_{oo} = K_{BB} \cdot K_x$

$K_{ii} = K_{CC} \cdot K_x$

$K_{ooi} = K_{BC} \cdot K_{BB} \cdot K_x^2$

$K_{iio} = K_{BC} \cdot K_{CC} \cdot K_x^2$

Following the unidirectional flux through the various forms of the allosteric pore without the assumption of slow catalytic steps is impractical. Hence the catalytic interconversions between the oligomeric states of the occupied pore are shown in Scheme 3. The interconversions of the symmetric conformational

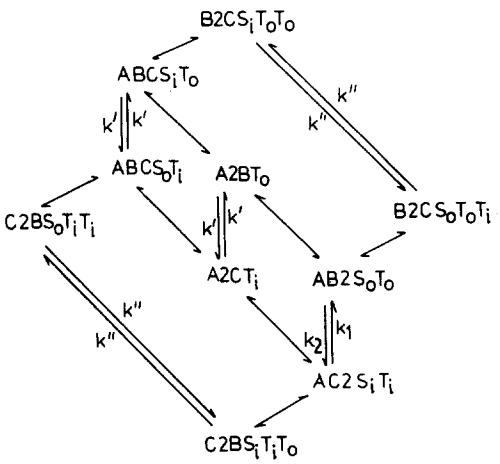

Scheme 3. This scheme shows the equilibria between the various forms of the allosteric pore and the proposed translocation events. The translocation rate constants for the stable pores (ABC, A2B and A2C) are symmetrical and given by k'. No shape change occurs in the conversion of $ABCS_iT_o$ to $ABCS_oT_i$, the only difference is that tracer exchange has taken place. A shape change occurs in the conversion of the AB2 to the AC2 pore and the translocation rates k_1 and k_2 are asymmetric. No shape change occurs in the interconversion of $B2CS_iT_oT_o$ and $B2CS_oT_oT_i$ but tracer exchange occurs within the pore. The rate constant for tracer exchange within the B2C and C2B pores is given by k''.

states must be symmetric and are assumed to be given by a single translocation constant k'. From the principle of a microscopic reversibility it can also readily be shown that the translocation rates for the doubly-occupied pores are asymmetric:

$$\frac{k_1}{k_2} = \frac{K_{BB}}{K_{CC}}$$

where k_1 and k_2 are the translocation rates for the pores doubly occupied from inside and outside, respectively. k'' is the rate constant for the tracer exchange

that occurs in the B2C and C2B pores. Hence, the net flux through the allosteric pore is:

$$U_{oi} - U_{io} = \frac{k'([S_o] - [S_i]) + vk'([S_o]^2 - [S_i]^2)}{D}$$

where D is the denominator in Eqn. 1 divided by T;

$$vk' = k_2 K_{oo} = k_1 K_{ii} = \frac{k_2 K_{BB}}{K_{CC}} K_{ii}$$

The unidirectional fluxes are:

$$U_{oi} = \frac{k'([S_o] + K_x[S_o] \cdot [S_i]) + vk'[S_o]^2 + k''(K_{ooi} \cdot [S_o]^2[S_i] + K_{iio}[S_i]^2[S_o])}{D}$$

$$U_{io} = \frac{k'([S_i] + K_x[S_o] \cdot [S_i]) + vk'[S_i]^2 + k''(K_{iio}[S_i]^2[S_o] + K_{ooi}[S_o]^2[S_i])}{D}$$

From these equations it is clear that, when the pore is doubly occupied from either outside or inside, transport will show negative cooperativity if K_{BB} and K_{CC} are less than 1 and positive cooperativity if K_{BB} and K_{CC} are greater than 1. To account for sugar transport in intact erythrocytes we assume that the interfaces between subunits are unstable in the doubly-occupied pore. Also, the CC interface is assumed to be more unstable than the BB interface and this introduces influx and efflux asymmetries in both K_m and V for the doubly-occupied pores. The overall asymmetry will be given by the ratio K_{BB}/K_{CC}:

$$\frac{K_{oo}}{K_{ii}} = \frac{k_1}{k_2} = \frac{K_{BB}}{K_{CC}}$$

In order to fit the allosteric pore equations to the data for sugar transport in intact erythrocytes we require estimates of seven independent parameters K_x, K_{BB}, K_{CC}, K_{BC}, k', vk', k''. For glucose $1/K_x = 1.2$, $K_{BB} = 0.156$, $K_{CC} = 0.031$, $K_{BC} = 0.24$, $k' = 0.3$ mM $\cdot$ s^{-1}, $vk' = 0.078$, $k'' = 4.0$ mM $\cdot$ s^{-1}.

The determination of apparent affinity constants requires computer analysis. Computer simulations of progress curves were carried out by the use of a numerical integration program. The parameter values were determined by trial and error and no attempt was made to refine the estimates with least-squares-fitting procedures.

For galactose, $1/K_x$ is higher than for glucose and equal to 8.33 mM. The translocation rates for the doubly-occupied pores are also higher than for glucose, $vk' = 0.0207$, $k'' = 7.0$ mM $\cdot$ s^{-1}. Other parameter values (the interface stability constants) are unaltered.

Combinations of low K/low V and high K/high V components in the equations for sugar flux will give barely detectable non-linearity in reciprocal plots and this is shown in Results.

Results

Zero trans experiments

In this procedure the *trans* concentration is kept at zero while the *cis* concentration is varied and consequently the *cis* saturation constant is obtained.

The data of Ginsburg and Stein [11] for galactose transport in red cells gave evidence of two K_m and two V values for net influx under zero *trans* conditions. However, their data are consistent with negative cooperativity. This is because at low concentrations sites of high affinity become saturated, but as the concentration is increase low-affinity sites are produced and there is a less steep rise to V. In reciprocal plots the most obvious feature will be the low saturation constant. The simulated values for the allosteric pore model are consistent with these findings. The simulated values for zero *trans* glucose influx are $K_{zt}^{oi} = 2.27$ mM and $V_{zt}^{oi} = 31.8$ mM · min^{-1} and can be compared with the published data for glucose and galactose transport in Table I. For galactose the simulated zero *trans* entry data and the experimental data give more evidence of non-Michaelis-Menten behaviour than for glucose. The simulated and experimental data give a better 2 K_m least-squares fit than a 1 K_m least-squares fit. If fitted to a 1 K_m process the operational K_m will slightly depend on the concentration range tested. The same will be true of exit.

Both glucose and galactose show asymmetry in the zero *trans* experiments with a high K_m, higher V for efflux than for influx. The allosteric pore model has been used to simulate an exit experiment for glucose similar to that of Karlish et al. [12] (Fig. 2). In this procedure cells are loaded with 80 mM glucose and the time course for exit is followed. The simulated time course also shows the changes in the fractional saturation of the pore by $AC2S_i2$ and $A2CS_i$. Initially, when the internal concentration is high the pores are doubly occupied and the exit rate (V) is high. As the concentration falls the fraction of singly-occupied pores increases. The operational K_m (from an integrated rate equation replot) is then $K_{zt}^{io} = 27$ mM, and $V_{zt}^{io} = 168$ mM · min^{-1}. This type of behaviour is typical of allosteric enzyme models where, depending upon occupancy, changed between high K/high V and low K/low V states occur. Increasing occupancy destabilizes the interfaces between subunits.

Equilibrium exchange

In equilibrium exchange $[S_o] = [S_i] = [S]$ and $[S]$ is varied. Under these conditions the unidirectional fluxes are measured with tracer and are equal for influx and efflux. Simulation of this experiment also demonstates a change from a low K/low V to a high K/high V state as the substrate concentration is increased (Fig. 3). At low concentrations the slow exchange predominates. The pore is predominantly in the form $ABCS_oS_i$ which has high affinity and a low translocation rate because all the interfaces between the subunits are stable. At high concentrations the fast exchange predominates. The pore here is predominately in the $B2CS_o2S_i$ and $C2BS_i2S_o$ forms which have unstable interfaces between the subunits and hence show low affinity but a high translocation rate. The overall effect is an exchange $K_m(K_{ee})$ of 26 mM and $V_{ee} = 233$ mM · min^{-1} with no detectable non-linearity.

Infinite cis and infinite trans experiments

In these experiments flux is measured when one surface of the membrane (*cis*) is saturated by substrate and the *trans* concentration is varied. In the infinite *cis* experiment the net flux from *cis* to *trans* is followed. In the infinite

TABLE I

SIMULATED AND EXPERIMENTAL DATA FOR SUGAR TRANSPORT IN HUMAN ERYTHROCYTES

A value for infinite *trans* galactose exit has not been experimentally determined. Therefore, the simulated value predicts the results of this experiment.

Experiment	Simulated glucose data		Simulated galactose data		Glucose data			Galactose data		
	K (mM)	V (mM · min^{-1})	K (mM)	V (mM · min^{-1})	K (mM)	V (mM · min^{-1})	Ref.	K (mM)	V (mM · min^{-1})	Ref.
Zero *trans* entry	2.27	32.8	29	60	1.6	36	10	31.7	28.6	11
Zero *trans* exit	27	168	239	327	25	129	12	249	255	
Infinite *cis* entry	3.8	—	25	—	2.8	—	14	25	—	11
Infinite *cis* exit	1.7	—	12	—	1.7	—	15	12	—	16
Infinite *trans* entry	3.4	123	24	167	1.7	174	11	21	239	13
Infinite *trans* exit	3.8	178	24	254	3.4	17	18 *	—	—	
Exchange	26	233	227	428	34	360	19	138	432	13

* 2°C.

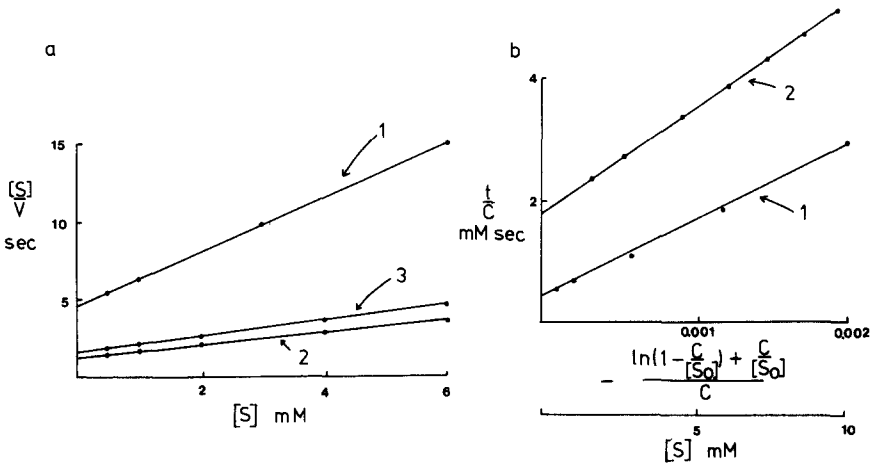

Fig. 1. (a) Simulated glucose transport data for (1) zero *trans* entry (2) infinite *trans* exit and (3) infinite *trans* entry. (b) Simulated glucose transport data for initial rates of infinite *cis* exit (1) and for infinite *cis* entry (2). The entry data are a simulated time course. The infinite *cis* K_m is equal to $[S_o]^2$ times the intercept on the abscissae. $[S_o]$ is the external concentration of glucose which is 60 mM. C is the internal concentration.

trans experiment the tracer flux from *trans* to *cis* is followed. The net influx through the allosteric pore when $[S_o] \to \infty$

$$U_{oi} - U_{io} = \frac{Vk'/K_{ooi}}{\frac{K_{oo}}{K_{ooi}} + [S_i]}$$

Applying a similar analysis to the infinite *cis* exit, infinite *trans* exit and infinite

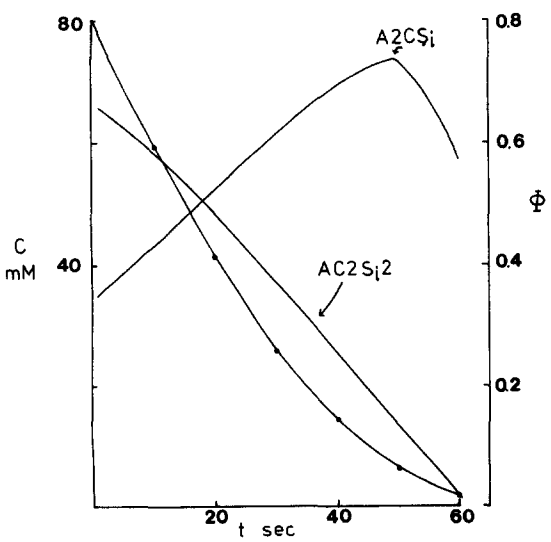

Fig. 2. A simulated zero *trans* exit experiment for 80 mM glucose (left axis). Also shown (right axis) is the fractional saturation (Φ) by $A2CS_i$ (singly occupied) and $AC2S_i2$ (doubly occupied) pores.

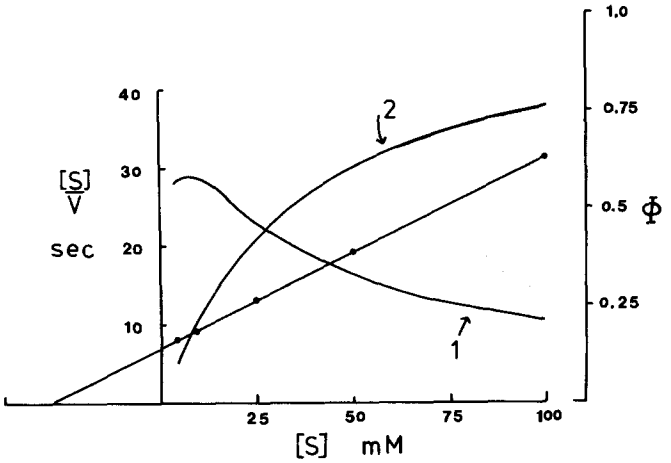

Fig. 3. A simulated glucose exchange experiment (left axis). Also shown (right axis) is the fractional saturation (Φ) by sites showing slow exchange (1) and fast exchange (2).

trans entry experiments give:

$$K_{ic}^{oi} = K_{ic}^{io} = K_{it}^{oi} = K_{it}^{io} = 1/K_x \cdot K_{BC}$$

This analysis indicates that the infinite *cis* and infinite *trans* K_m values are symmetric. In practice computer simulations show that the infinite *cis* K_m values are slightly less than $1/K_x \cdot K_{BC}$. This is because some of the sites are in the $ABCS_oS_i$ form which has high affinity.

The computed values for the glucose infinite *cis* and infinite *trans* experiments for entry and exit, respectively, are K_{ic}^{oi} = 3.8 mM, K_{it}^{oi} = 3.4 mM, K_{ic}^{io} = 1.7 mM, K_{it}^{io} = 3.8 mM. These values are compared with the published data in Table I.

Discussion

General properties of the allosteric pore

Pore models for sugar transport are consistent with the evidence for a water-filled sugar-dependent transport route across the membrane. Sugar-dependent increases in membrane water have been noted [19]. The possibility of the formation of a disorganized water layer around certain steroids when they interact with the glucose transport system has been reported by Lacko et al. [20]. Bowman and Levitt [21] have demonstrated that occupation of the glucose transporter by a series of 4—6 carbon polyols is inversely realted to their molecular size and these authors have therefore suggested that this may be related to the ability of these compounds to enter a pore.

The allosteric pore can account for saturation phenomena in transport. If the cooperativity is negative then the reciprocal plots will appear linear. The allosteric pore is different from the carrier model for transport in that the conformational changes are substrate-induced, thus phenomena such as counterflow and *trans* acceleration are due to *trans* destabilization of the protein subunits in the pore (a gating phenomenon, see below) rather than to

a conformational change involving back-flux of an empty carrier.

The difference between substrate-dependent and substrate-independent conformational changes will be seen in inactivation experiments. For the allosteric pore model differences in the susceptibility of exchange and net flux to inactivation are predicted because transport cycles exist without the empty transport system as an intermediate. The carrier model predicts that exchange and net flux should be equally effected by inactivators since each transport cycle involves the empty carrier as an intermediate. Differences in inactivation of exchange and net flux of sugars have been noted [19]. Also, the lower activation energy for exchange than for net flux is more consistent with a gating pore than with a carrier model [19].

Besides these general considerations, and the properties of the allosteric pore model that enable it to be fitted to all the kinetic data, the present model has additional features that may form the basis of future experiments. Although for a single substrate no evidence of non-linearity of kinetic plots will be discernable this may not always be the case when a substrate and an inhibitor interact with the transport system. In fact, the inhibition of sugar transport by certain steroids gives parabolic inhibition plots [20]. The interaction of 1-fluoro-2,4-dinitrobenzene with sugar transport has been reported to be a second-order process [22]. In addition, because K_{BB} is much greater than K_{CC} an inhibitor that reduces the number of internal doubly-occupied pores (stabilizes the CC interface) may be expected to produce uncompetitive inhibition of sugar exit but produce little or no change in influx. This type of behaviour has been noted for the effect of ^2H_2O in whole cells [23]. The K_m and V for efflux are both decreased equally by this agent while K/V remains constant.

The molecular basis for K_{BB} being greater than K_{CC} may be that the pore gates (protein subunits) are also controlled by modifier proteins of the cytoskeletal network. This is consistent with the observation that mild proteolytic digestion of the inner membrane surface of erythrocyte ghosts results in a marked inhibition of sugar exit [24]. A more easily opened gate at the inner surface may account for the specificity differences observed for glucose analogues at internal and at external sites [25].

Gating phenomena in transport

The allosteric pore model may be applicable to other transport systems. It seems useful to regard the interfaces between subunits not only as substrate binding sites but also as gates which impede the flux of materials that do not cause a substrate-dependent opening of the pore. This is shown diagrammatically in Scheme 1.

Modifiers of transport in some circumstances may be cosubstrates. For example, if a high-affinity (tightly bound) poorly transported substrate and a low-affinity substrate interact then the pore may be converted into an open conformational state by the poorly transported substrate, and this may accelerate the flux of the low-affinity substrate. It would be of interest to determine whether ion transport gating may have an explanation in terms of the allosteric pore. An additional factor to consider here would be the effect

of membrane potential on protein subunit aggregation within the membrane pores.

Acknowledgements

This work is supported by a grant from the British Diabetic Association for which we are grateful. We are grateful to Dr. R.J. Naftalin for helpful comments and for a critical reading of the manuscript.

References

1 Widdas, W.F. (1954) J. Physiol. 125, 163—180
2 Naftalin, R.J. (1970) Biochim. Biophys. Acta 211, 65—78
3 Lieb, W.R. and Stein, W.D. (1970) Biophys. J. 10, 587—609
4 Lefevre, P.G. (1973) J. Membrane Biol. 11, 1—19
5 Geck, P. (1971) Biochim. Biophys. Acta 241, 462—472
6 Regen, D.M. and Tarpley, H.L. (1974) Biochim. Biophys. Acta 339, 218—233
7 Eilam, Y. (1975) Biochim. Biophys. Acta 401, 349—363
8 Koshland, D.E., Jr. (1970) in The Enzymes (Boyer, P.D., ed.), 3rd edn., Vol. 1, pp. 341—396, Academic Press, New York
9 Koshland, D.E., Jr., Nemethy, G. and Filmer, D. (1966) Biochemistry 5, 365—385
10 Lacko, L., Wittke, B. and Kromphardt, H. (1972) Eur. J. Biochem. 25, 447—454
11 Ginsburg, H. and Stein, W.D. (1975) Biochim. Biophys. Acta 382, 353—368
12 Karlish, S.J.D., Lieb, W.R., Ram, D. and Stein, W.D. (1972) Biochim. Biophys. Acta 255, 126—132
13 Ginsburg, H. and Ram, D. (1975) Biochim. Biophys. Acta 382, 369—376
14 Hankin, B.L., Lieb, W.R. and Stein, W.D. (1972) Biochim. Biophys. Acta 288, 114—126
15 Sen, A.K. and Widdas, W.F. (1962) J. Physiol. 160, 392—403
16 Krupka, R.M. (1972) Biochemistry 10, 1143—1147
17 Baker, G.F. and Naftalin, R.J. (1979) Biochim. Biophys. Acta 550, 474—484
18 Eilam, Y. (1975) Biochim. Biophys. Acta 401, 364—369
19 Naftalin, R.J. and Holman, G.D. (1977) in Membrane Transport in Red Cells (Ellory, J.C. and Lew, V.L., eds.), pp. 257—299, Academic Press, London
20 Lacko, L., Wittke, B. and Lacko, I. (1977) J. Cell. Physiol. 90, 161—168
21 Bowman, R.J. and Levitt, D.G. (1977) Biochim. Biophys. Acta 466, 68—83
22 Shimmin, E.R.A. and Stein, W.D. (1970) Biochim. Biophys. Acta 211, 308—312
23 Baker, G.F. and Naftalin, R.J. (1979) J. Physiol. 280, 25 P
24 Masiak, S.J. and LeFevre, P.G. (1977) Biochim. Biophys. Acta 465, 371—377
25 Barnett, J.E.G., Holman, G.D., Chalkley, R.A. and Munday, K.A. (1975) Biochem. J. 145, 417—429